ELSEVIER

Chemical Engineering Journal 83 (2001) 191–200

Chemical Engineering Journal

www.elsevier.com/locate/cej

Methanol synthesis in a fluidized-bed reactor coupled with an external heat exchanger The effect of feedback deformation

Bolesław Tabiś

Institute of Chemical Engineering and Physical Chemistry, Cracow University of Technology, 31-155 Kraków, 24 Warszawska, Poland

Received 18 February 2000; received in revised form 26 June 2000; accepted 30 August 2000

Abstract

Quantitative analysis of the steady states multiplicity, linear stability and the yield of a fluidized-bed reactor for the low pressure methanol synthesis has been performed. The reactor coupled with an external heat exchanger has been considered. Particular attention has been focused on the analysis of the effect of external feedback deformation on the stationary properties of this configuration. The obtained results show a significant influence of operational parameters on the yield of the reactor. The existence of maxima of the yield has been proven. © 2001 Elsevier Science B.V. All rights reserved.

Keywords: Methanol; Fluidized-bed reactor; Heat exchanger

1. Introduction

Methanol belongs to the most important semiproducts of organic synthesis. The significance of methanol has motivated numerous studies whose aim was to improve the efficiency of the conventional fixed-bed reactor synthesis or to develop and evaluate new processes [1–5]. One of these new possibilities is the fluidized-bed technology [6–9].

Hydrodynamic and thermal properties of the fluidized bed are the source of inner channels of thermal feedback and generate in this way autothermal structure. It appears that a single fluidized-bed reactor can ensure an autothermal way of methanol synthesis [6,7].

The phenomenon of autothermicity is the source of multiple steady states of the reactor. It results from the studies published up to the present that the region of the existence of multiple steady states to a large extent overlaps the operational conditions of industrial reactors. Technologically advantageous conversion degrees correspond only to upper steady states. Though to achieve those upper steady states, the temperature of the feed has to be raised which increases the operation costs. It appears though that there exits a possibility to choose such autothermal configurations so that this difficulty is overcome. One of the solutions is to install an external heat exchanger to preheat the feed. Such autothermal structure is characterised by both internal and external channels of heat feedback. Internal coupling results from the structure of the fluidized bed and the external one is ensured by the presence of the autothermal heat exchanger (Fig. 1).

The autothermal system presented in Fig. 1 can be operated according to the so-called simple or deformed scheme. The deformation of external coupling is caused by an additional stream of reagents of temperature T_0 which is fed in the amount of F_{m0}. To this date only in the work [8] there were discussed the results of preliminary studies on the basic non-linear stationary properties of the autothermal structure with an external heat exchanger.

The present work is more systematic and comprehensive since the developed set of model equations makes it possible to employ any continuation method for the determination of steady state hysteresis branches for the system of Fig. 1 with simultaneous examination of the linear stability of these states. On the basis of the obtained equations, the continuation of turning points was also carried out. The essential goal of the work is related to the determination of the yield of the reactor for each point lying in the steady state curve. Results of studies of this kind have not been published by any author dealing with the modelling and analysis of fluidized-bed reactor operation up to the present. On the basis of such results optimum conditions of synthesis can be determined.

2. Stoichiometry, equilibrium and process kinetics

According to a commonly accepted view [10] it was assumed that the low pressure synthesis of methanol proceeds

1385-8947/01/$ – see front matter
PII: S1385-8947(00)00254-0

Nomenclature

a_i	dimensionless model parameters
a_p	fugacity (atm)
a_q	heat transfer area per unit volume of a bed (m^{-1})
A_i	ith component of reaction mixture
A_q	heat transfer area in an autothermal heat exchanger (m^2)
Ar	Archimedes number
B_i, B_{ij}	model parameters determining the intensity of interphase heat and mass transfer
c_g, c_z	specific heat of gas and solid particles ($kJ\,kg^{-1}\,K^{-1}$)
C_i^j	concentration of the ith component in the jth phase ($kmol\,m^{-3}$)
C_{if}	feed concentration of the ith reactant ($kmol\,m^{-3}$)
d_b	diameter of the gas bubble (m)
f_i	fugacity coefficient of the ith component
F_{met}	productivity of the reactor per unit cross-section of a fluidized bed ($kg\,m^{-2}\,s^{-1}$)
F_{mg}	mass flow rate of gas ($kg\,s^{-1}$)
h	current coordinate of height in the fluidized bed (m)
Δh_i	enthalpy of the ith chemical reaction under synthesis conditions ($kJ\,kmol^{-1}$)
H	dynamic height of the bed (m)
k	codimension of singularity
$k_i(T)$	rate constant of the ith chemical reaction
k_q	overall heat transfer coefficient ($kJ\,m^{-2}\,s^{-1}\,K^{-1}$)
K_{api}	thermodynamic equilibrium constant for the ith chemical reaction
K_{fi}	quotient of thermodynamic and approximate equilibrium constants for the ith reaction
K_i	constant of adsorption equilibrium for the ith component
K_{pi}	approximate equilibrium constant for the ith reaction
l_f	fluidization ratio, $l_f = u_0/u_{mf}$
M_i	molar mass of the ith component ($kg\,kmol^{-1}$)
$\bar{M}$	mean molar mass ($kg\,kmol^{-1}$)
n_i	number of moles of the ith component (kmol)
p, p_i	total pressure and partial pressure of the ith component (atm)
$\dot{Q}$	rate of heat transfer ($kJ\,s^{-1}$)
Q_i	model parameters determining intensity of overall heat transfer (s^{-1})
r_i	rate of the ith chemical reaction ($kmol\,s^{-1}\,m^{-3}$)
R	gas constant ($kJ\,kmol^{-1}\,K^{-1}$)
S	cross-section of a fluidized bed (m^2)
t	time (s)
T_0	temperature of the additional feed stream (K)
T^j	temperature of the jth phase (K)
T_f, T_q	temperatures of feed and cooling media (K)
ΔT_m	mean difference of temperatures (K)
u_0	current superficial gas velocity ($m\,s^{-1}$)
u_b	rise velocity of bubbles ($m\,s^{-1}$)
u_e	velocity of gas in the emulsion phase ($m\,s^{-1}$)
u_{mf}	superficial gas velocity at minimum fluidization conditions ($m\,s^{-1}$)
x	vector of state
y_i	molar fraction of the ith component
y_{i0}	molar fraction of the ith component in the feed stream
z	dimensionless bed height

Greek symbols

α_i	degree of conversion of the ith reference reactant
α_q^{ij}	heat exchange coefficient between the phase i, j ($kJ\,m^{-3}\,s^{-1}\,K^{-1}$)
β_q^{ij}	gas exchange coefficient between the phase i, j (s^{-1})
β_z^{ij}	solid particles exchange coefficient between the phase i, j (s^{-1})
δ	volumetric fraction of bubbles in the fluidized bed
ε_{mf}	void fraction in the emulsion phase at minimum fluidization conditions
η	degree of deformation of the external autothermal feedback
ρ_g, ρ_z	density of gas and solid particles, respectively ($kg\,m^{-3}$)

Subscripts

0	refers to the stream deforming the external thermal feedback
f	refers to feed stream
p, s	refers to reaction products and substrates, respectively

Superscripts

b, e	refers to bubble and emulsion phase, respectively

according to the scheme

$$CO + 2H_2 \rightleftarrows CH_3OH \quad (1a)$$

$$CO_2 + 3H_2 \rightleftarrows CH_3OH + H_2O \quad (1b)$$

$$CO_2 + H_2 \rightleftarrows CO + H_2O \quad (1c)$$

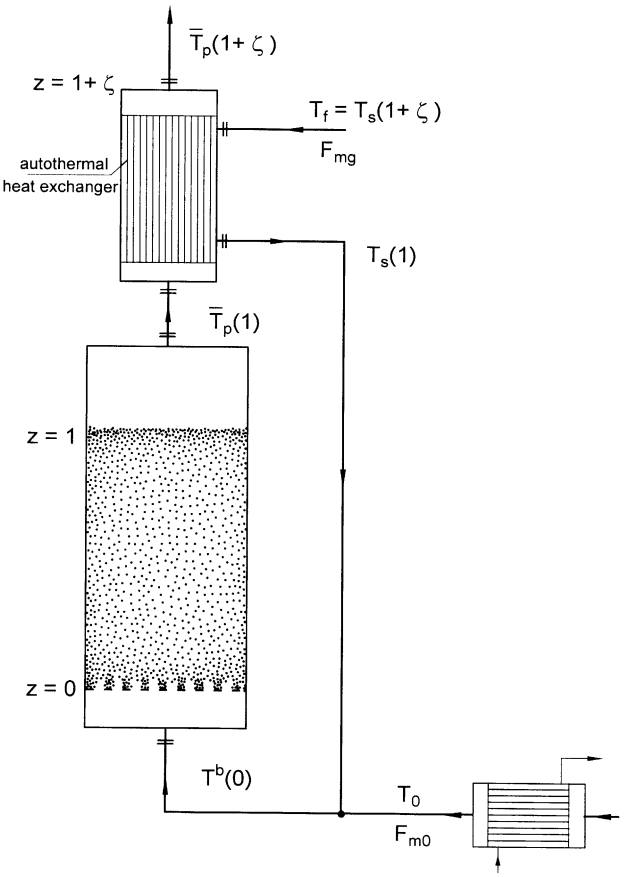

Fig. 1. A fluidized-bed reactor with an external heat exchanger.

To simplify the notation let us denote the components of the reaction mixture as follows

A_1	A_2	A_3	A_4	A_5	A_6
CO	CO_2	H_2	CH_3OH	H_2O	inerts

If the conversion degrees of the reference components A_1 and A_2 are defined by the expressions

$$\alpha_1 = \frac{\Delta n_1}{n_{01}}, \qquad \alpha_2 = \frac{\Delta n_2}{n_{02}} \tag{2}$$

then the actual composition of the reaction mixture will be described by the following relationships

$$y_1 = \frac{y_{01}(1-\alpha_1)}{1-2y_{01}\alpha_1-2y_{02}\alpha_2}, \quad y_2 = \frac{y_{02}(1-\alpha_2)}{1-2y_{01}\alpha_1-2y_{02}\alpha_2},$$
$$y_3 = \frac{y_{03}-2y_{01}\alpha_1-3y_{02}\alpha_2}{1-2y_{01}\alpha_1-2y_{02}\alpha_2}, \quad y_4 = \frac{y_{04}+y_{01}\alpha_1+y_{02}\alpha_2}{1-2y_{01}\alpha_1-2y_{02}\alpha_2},$$
$$y_5 = \frac{y_{05}+y_{02}\alpha_2}{1-2y_{01}\alpha_1-2y_{02}\alpha_2}, \quad y_6 = \frac{y_{06}}{1-2y_{01}\alpha_1-2y_{02}\alpha_2} \tag{3}$$

The values of equilibrium conversion degrees α_1^* and α_2^* and hence the equilibrium composition are calculated by solving a set of two non-linear equations, namely

$$K_{pj}(\alpha_1^*, \alpha_2^*)K_{fj} - K_{apj}(T) = 0 \quad (j = 1, 2) \tag{4}$$

where

$$K_{p1} = \frac{p_4}{p_1 p_3^2}, \qquad K_{p2} = \frac{p_4 p_5}{p_2 p_3^3} \tag{5}$$

and

$$K_{f1} = \frac{f_4}{f_1 f_3^2}, \qquad K_{f2} = \frac{f_4 f_5}{f_2 f_3^3} \tag{6}$$

whereas $p_i = p y_i(\alpha_1, \alpha_2)$ $(i = 1, \ldots, 5)$.

To describe the rates of chemical reactions (1a)–(1c), a kinetic model proposed by Takagawa and Ohsugi [11] was assumed. The expressions determining the rates of all the three chemical reactions (1a)–(1c) which can proceed during the synthesis assume the following form

$$r_1 = k_1(T)(a_{p1}a_{p3}^b)^{c_1}\frac{1-(K_{p1}K_{f1}/K_{ap1})^{c_2}}{1+a_{p2}K_2+a_{p5}K_5} (\text{kmol m}^{-3}\,\text{s}^{-1}) \tag{7a}$$

$$r_2 = k_2(T)a_{p2}\frac{1-K_{p2}K_{f2}/K_{ap2}}{1+a_{p5}K_5} (\text{kmol m}^{-3}\,\text{s}^{-1}) \tag{7b}$$

$$r_3 = k_3(T)a_{p3}\frac{1-K_{p3}K_{f3}}{K_{ap3}} (\text{kmol m}^{-3}\text{s}^{-1}) \tag{7c}$$

where $a_i = p_i f_i$ $(i = 1, \ldots, 5)$.

After changing the units of time, volume and energy from hours, litres and calories [11] into seconds, cubic metres and joules, respectively, the kinetic constants occurring in the expressions (7a)–(7c) are calculated according to the relationships

$$k_1(T) = 2.86 \times 10^3 \exp\left(\frac{-69460}{RT}\right) \tag{8a}$$

$$k_2(T) = 6.47 \times 10^3 \exp\left(\frac{-62760}{RT}\right) \tag{8b}$$

$$k_3(T) = 3.47 \times 10^8 \exp\left(\frac{-120500}{RT}\right) \tag{8c}$$

$$K_2(T) = 1.86 \times 10^{-9} \exp\left(\frac{75730}{RT}\right) \tag{8d}$$

$$K_5(T) = 1.06 \times 10^{-7} \exp\left(\frac{69870}{RT}\right) \tag{8e}$$

where $R = 8.3143\,\text{kJ kmol}^{-1}\,\text{K}^{-1}$, whereas $b = 2.5$; $c_1 = 0.35$ and $c_2 = 0.8$.

The thermodynamic constants K_{p3} and K_{f3} in Eq. (7c) are determined by the expressions

$$K_{p3} = \frac{p_1 p_5}{p_2 p_3}, \qquad K_{f3} = \frac{f_1 f_5}{f_2 f_3}$$

3. Model of the process

For the purpose of non-linear analysis, namely for the continuation of steady states and turning points as well as to study the linear dynamics of steady states, a two-phase model of methanol synthesis in a fluidized bed was created. Homogeneity of concentration fields and the temperature in the emulsion phase and plug flow of the bubbles were assumed.

The dynamics of the emulsion phase is described by the equations

$$\frac{\mathrm{d}\alpha_1^{\mathrm{e}}}{\mathrm{d}t} = -a_{21}\alpha_1^{\mathrm{e}} + B_{11}\int_0^1 (\alpha_1^{\mathrm{b}} - \alpha_1^{\mathrm{e}})\,\mathrm{d}z + \frac{a_3}{C_{1\mathrm{f}}}(r_1 - r_3) \quad (9a)$$

$$\frac{\mathrm{d}\alpha_2^{\mathrm{e}}}{\mathrm{d}t} = -a_{22}\alpha_2^{\mathrm{e}} + B_{12}\int_0^1 (\alpha_2^{\mathrm{b}} - \alpha_2^{\mathrm{e}})\,\mathrm{d}z + \frac{a_3}{C_{2\mathrm{f}}}(r_2 + r_3) \quad (9b)$$

$$\frac{\mathrm{d}T^{\mathrm{e}}}{\mathrm{d}t} = a_5(T^{\mathrm{b}}(0) - T^{\mathrm{e}}) + a_4\sum_{i=1}^{3}\Delta h_i r_i - B_2\int_0^1 (T^{\mathrm{e}} - T^{\mathrm{b}})\,\mathrm{d}z - Q_1(T^{\mathrm{e}} - T_{\mathrm{q}}) \quad (9c)$$

Objects such as non-isothermal gas–solid fluidized-bed reactors are characterised by slow changes in the emulsion temperature as compared to several hundred or even several thousand faster changes in the temperature and concentration in the bubbles. It is caused by a high thermal inertia of solid particles. In other words, the resultant dynamics of the entire fluidized bed is affected by the high thermal inertia of the emulsion phase. An assumption of the pseudo-steady state of the bubble phase is then introduced. A comprehensive and extensive discussion explaining the introduction of such an assumption was presented in an earlier work [12]. The equations for the bubble phase assume then the following form

$$\frac{\mathrm{d}\alpha_1^{\mathrm{b}}}{\mathrm{d}z} = B_{31}(\alpha_1^{\mathrm{e}} - \alpha_1^{\mathrm{b}}) \quad (10a)$$

$$\frac{\mathrm{d}\alpha_2^{\mathrm{b}}}{\mathrm{d}z} = B_{32}(\alpha_2^{\mathrm{e}} - \alpha_2^{\mathrm{b}}) \quad (10b)$$

$$\frac{\mathrm{d}T^{\mathrm{b}}}{\mathrm{d}z} = B_4(T^{\mathrm{e}} - T^{\mathrm{b}}) - Q_2(T^{\mathrm{b}} - T_{\mathrm{q}}) \quad (10c)$$

with the initial conditions

$$\alpha_1^{\mathrm{b}}(0) = \alpha_2^{\mathrm{b}}(0) = 0 \quad (11a)$$

$$T^{\mathrm{b}}(0) = T_0^{\mathrm{b}} \quad (11b)$$

where $z = (h/H) \in [0,\ 1]$.

The following reduced parameters have been introduced into Eqs. (9a)–(9c) and (10a)–(10c) to simplify the notation:

$$a_1 = \frac{\rho_{\mathrm{g}} c_{\mathrm{g}}}{\rho_{\mathrm{z}} c_{\mathrm{z}}}, \qquad a_{2,i} = \frac{u_{\mathrm{e}} C_{i\mathrm{f}}}{H} \quad (i = 1, 2),$$

$$a_3 = \frac{1 - \varepsilon_{\mathrm{mf}}}{\varepsilon_{\mathrm{mf}}}, \qquad a_4 = \frac{1 - \varepsilon_{\mathrm{mf}}}{(1 - \varepsilon_{\mathrm{mf}} + \varepsilon_{\mathrm{mf}}/a_1)\rho_{\mathrm{z}} c_{\mathrm{z}}},$$

$$a_5 = \frac{\varepsilon_{\mathrm{mf}} u_{\mathrm{e}}}{H[(1 - \varepsilon_{\mathrm{mf}})a_1 + \varepsilon_{\mathrm{mf}}]},$$

$$B_{1i} = \frac{\delta\beta_{\mathrm{g}i}^{\mathrm{be}}}{(1 - \delta)\varepsilon_{\mathrm{mf}}} \quad (i = 1, 2),$$

$$B_2 = \frac{\delta}{(1 - \delta)(1 - \varepsilon_{\mathrm{mf}} + \varepsilon_{\mathrm{mf}}/a_1)}\left(\frac{\alpha_{\mathrm{q}}^{\mathrm{be}}}{\rho_{\mathrm{z}} c_{\mathrm{z}}} + \beta_{\mathrm{z}}^{\mathrm{be}}\right),$$

$$B_{3i} = \frac{H}{u_{\mathrm{b}}}\beta_{\mathrm{g}i}^{\mathrm{be}} \quad (i = 1, 2), \qquad B_4 = \frac{H}{u_{\mathrm{b}}}\left(\frac{\alpha_{\mathrm{q}}^{\mathrm{be}}}{\rho_{\mathrm{z}} c_{\mathrm{z}}} + \beta_{\mathrm{z}}^{\mathrm{be}} a_1\right)$$

$$Q_1 = \frac{a_{\mathrm{q}} k_{\mathrm{q}}}{(1 - \varepsilon_{\mathrm{mf}} + \varepsilon_{\mathrm{mf}}/a_1)\rho_{\mathrm{z}} c_{\mathrm{z}}}, \qquad Q_2 = \frac{H}{u_{\mathrm{b}}}\frac{a_{\mathrm{q}} k_{\mathrm{q}}}{\rho_{\mathrm{z}} c_{\mathrm{z}}}$$

The interchange coefficients and other parameters determining the hydrodynamics of the fluidized bed occurring in the model were calculated according to the Kunii–Levenspiel model [13,14]. The diameter of the gas bubbles was calculated as an integral mean employing the function $d_{\mathrm{b}}(h)$ given by Kobayashi [15]. The bed porosity in the conditions of minimum fluidization $\varepsilon_{\mathrm{mf}}$ was calculated according to the proposition of Broadhurst and Becker [16]

$$\varepsilon_{\mathrm{mf}} = 0.568\,Ar^{-0.029}\left(\frac{\rho_{\mathrm{g}}}{\rho_{\mathrm{z}}}\right)^{0.021}$$

The integration of Eqs. (10a)–(10c) with the conditions (11a) and (11b) gives

$$\alpha_i^{\mathrm{b}}(z) = \alpha_i^{\mathrm{e}}[1 - \exp(-B_{3i}z)] \quad (i = 1, 2) \quad (12a,b)$$

$$T^{\mathrm{b}}(z) = \frac{B_4 T^{\mathrm{e}} + Q_2 T_{\mathrm{q}}}{B_4 + Q_2} + \left[T^{\mathrm{b}}(0) - \frac{B_4 T^{\mathrm{e}} + Q_2 T_{\mathrm{q}}}{B_4 + Q_2}\right] \times \exp(-(B_4 + Q_2)z) \quad (12c)$$

After the substitution of the functions $\alpha_1^{\mathrm{b}}(z)$, $\alpha_2^{\mathrm{b}}(z)$ and $T(z)$ into Eqs. (9a)–(9c) and after the evaluation of the integrals we obtain the final form of the equations, namely

$$\frac{\mathrm{d}\alpha_1^{\mathrm{e}}}{\mathrm{d}t} = -a_{21}\alpha_1 + \varphi_1(\alpha_1^{\mathrm{e}}) + \frac{a_3}{C_{1\mathrm{f}}}(r_1 - r_3) = f_1(\alpha_1^{\mathrm{e}}, \alpha_2^{\mathrm{e}}, T^{\mathrm{e}}) \quad (13a)$$

$$\frac{\mathrm{d}\alpha_2^{\mathrm{e}}}{\mathrm{d}t} = -a_{22}\alpha_2 + \varphi_2(\alpha_2^{\mathrm{e}}) + \frac{a_3}{C_{2\mathrm{f}}}(r_2 + r_3) = f_2(\alpha_1^{\mathrm{e}}, \alpha_2^{\mathrm{e}}, T^{\mathrm{e}}) \quad (13b)$$

$$\frac{\mathrm{d}T^{\mathrm{e}}}{\mathrm{d}t} = a_5(T^{\mathrm{b}}(0) - T^{\mathrm{e}}) - \varphi_3(T^{\mathrm{e}}) + a_4\sum_{i=1}^{3} r_i(-\Delta h_i) - Q_1(T^{\mathrm{e}} - T_{\mathrm{q}}) = f_3(\alpha_1^{\mathrm{e}}, \alpha_2^{\mathrm{e}}, T^{\mathrm{e}}) \quad (13c)$$

where

$$\varphi_i(\alpha_i^{\mathrm{e}}) = \frac{B_{1i}}{B_{3i}}\alpha_i^{\mathrm{e}}[\exp(-B_{3i}) - 1] \quad (i = 1, 2) \tag{14a,b}$$

$$\varphi_3(T^{\mathrm{e}}) = \frac{B_2}{B_4 + Q_2} \times \left[Q_2(T^{\mathrm{e}} - T_{\mathrm{q}}) + \left(T^{\mathrm{b}}(0) - \frac{B_4 T^{\mathrm{e}} + Q_2 T_{\mathrm{q}}}{B_4 + Q_2} \right) \times (\exp(-(B_4 + Q_2)) - 1) \right] \tag{14c}$$

It results from Fig. 1 that the temperature of the fluidizing agent fed under the gas distributor in the reactor $T^{\mathrm{b}}(0)$ is equal to the temperature of the bubble phase for the co-ordinate $z = 0$. The value of $T^{\mathrm{b}}(0)$ depends on the temperature of the preheated feed $T_{\mathrm{s}}(1)$ and on the presence of an additional stream of reagents of the amount F_{m0} and the temperature T_0. This additional stream can come from recirculation of unreacted feed, for example. In the work it was shown that it can also be used to control the temperature in the entire autothermal system by means of an additional heat exchanger, marked with a thin line in Fig. 1. At $F_{\mathrm{m0}} > 0$ we have the case of the external autothermal feedback deformation. The type of this deformation is determined by two parameters, namely by the deformation degree η and the deformation direction, the measure of which is the relation between T_0 and T_{f}. If $T_0 < T_{\mathrm{f}}$ then we will have a "negative" direction, whereas for $T_0 > T_{\mathrm{f}}$, a "positive" one. The degree of the deformation η is defined by the expression

$$\eta = \frac{F_{\mathrm{m0}} c_{\mathrm{g0}}}{F_{\mathrm{mg}} c_{\mathrm{gs}} + F_{\mathrm{m0}} c_{\mathrm{g0}}} \tag{15}$$

The presence of the additional stream of reagents makes $T^{\mathrm{b}}(0) \neq T_{\mathrm{s}}(1)$. Then the temperature $T^{\mathrm{b}}(0)$ has to be calculated from the heat balance

$$F_{\mathrm{mg}} c_{\mathrm{gs}} T_{\mathrm{s}}(1) + F_{\mathrm{m0}} c_{\mathrm{g0}} T_0 = (F_{\mathrm{mg}} c_{\mathrm{gs}} + F_{\mathrm{m0}} c_{\mathrm{g0}}) T^{\mathrm{b}}(0) \tag{16}$$

whence

$$T^{\mathrm{b}}(0) = \eta T_0 + (1 - \eta) T_{\mathrm{s}}(1) \tag{17}$$

The presence of the autothermal heat exchanger introduces an additional equation, namely

$$\psi(T^{\mathrm{e}}, T_{\mathrm{s}}(1)) = T_{\mathrm{f}} - T_{\mathrm{s}}(1 + \zeta) = 0 \tag{18}$$

The unknown value of the temperature $T_{\mathrm{s}}(1 + \zeta)$ we shall evaluate from the equation of the heat balance of the autothermal heat exchanger

$$\dot{Q} = F_{\mathrm{mg}} c_{\mathrm{gs}} [T_{\mathrm{s}}(1) - T_{\mathrm{s}}(1 + \zeta)] \tag{19}$$

whence

$$T_{\mathrm{s}}(1 + \zeta) = T_{\mathrm{s}}(1) - \frac{\dot{Q}}{F_{\mathrm{mg}} c_{\mathrm{gs}}} \tag{20}$$

The equation $\psi(T^{\mathrm{e}}, T_{\mathrm{s}}(1)) = 0$ will then assume the form

$$\psi(T^{\mathrm{e}}, T_{\mathrm{s}}(1)) = T_{\mathrm{f}} - T_{\mathrm{s}}(1) + \frac{\dot{Q}}{F_{\mathrm{mg}} c_{\mathrm{gs}}} = 0 \tag{21}$$

The rate of heat exchange in the external "autothermal" exchanger is determined by the known kinetic equation

$$\dot{Q} = A_{\mathrm{q}} k_{\mathrm{q}} \Delta T_{\mathrm{m}} \tag{22}$$

where

$$\Delta T_{\mathrm{m}} = \frac{[\bar{T}_{\mathrm{p}}(1 + \zeta) - T_{\mathrm{f}}] - [\bar{T}_{\mathrm{p}}(1) - T_{\mathrm{s}}(1)]}{\ln[(\bar{T}_{\mathrm{p}}(1 + \zeta) - T_{\mathrm{f}})/(\bar{T}_{\mathrm{p}}(1) - T_{\mathrm{s}}(1))]} \tag{23}$$

If the heat exchanger is operated adiabatically then the heat of the reaction products is taken in it by the feed only, that is to say

$$(F_{\mathrm{mg}} + F_{\mathrm{m0}}) c_{\mathrm{gp}} [\bar{T}_{\mathrm{p}}(1) - \bar{T}_{\mathrm{p}}(1 + \zeta)] = F_{\mathrm{mg}} c_{\mathrm{gs}} [T_{\mathrm{s}}(1) - T_{\mathrm{f}}] \tag{24}$$

Hence we evaluate $\bar{T}_{\mathrm{p}}(1 + \zeta)$

$$\bar{T}_{\mathrm{p}}(1 + \zeta) = \bar{T}_{\mathrm{p}}(1) - \xi T_{\mathrm{s}}(1) + \xi T_{\mathrm{f}} \tag{25}$$

where

$$\xi = \frac{F_{\mathrm{mg}} c_{\mathrm{gs}}}{(F_{\mathrm{mg}} + F_{\mathrm{m0}}) c_{\mathrm{gp}}} \tag{26}$$

If $c_{\mathrm{gs}} = c_{\mathrm{gp}} = c_{\mathrm{g0}}$, which is close to the reality for the analysed process, then

$$\xi = \frac{F_{\mathrm{mg}}}{F_{\mathrm{mg}} + F_{\mathrm{m0}}}, \qquad \eta = \frac{F_{\mathrm{m0}}}{F_{\mathrm{mg}} + F_{\mathrm{m0}}} \tag{27}$$

and

$$\xi = 1 - \eta \tag{28}$$

In the light of the above relationships the mean temperature difference in the autothermal heat exchanger is equal to

$$\Delta T_{\mathrm{m}} = \frac{\eta [T_{\mathrm{s}}(1) - T_{\mathrm{f}}]}{\ln[(\bar{T}_{\mathrm{p}}(1) - (1 - \eta) T_{\mathrm{s}}(1) - \eta T_{\mathrm{f}})/(\bar{T}_{\mathrm{p}}(1) - T_{\mathrm{s}}(1))]} \tag{29}$$

Eventually, the equation $\psi(T^{\mathrm{e}}, T_{\mathrm{s}}(1)) = 0$ will assume the form

$$\psi(T^{\mathrm{e}}, T_{\mathrm{s}}(1)) = T_{\mathrm{f}} - T_{\mathrm{s}}(1) + \frac{A_{\mathrm{q}} k_{\mathrm{q}}}{F_{\mathrm{mg}} c_{\mathrm{gs}}} \Delta T_{\mathrm{m}}(T_{\mathrm{s}}(1)) = 0 \tag{30}$$

The quantity $\bar{T}_{\mathrm{p}}$ denotes the mean temperature of the product stream leaving the bed. Let us evaluate it as the weighted mean according to the fraction of the fluidizing agent coming from the bubble and emulsion phases, namely

$$\delta u_{\mathrm{b}} T^{\mathrm{b}}(1) + (1 - \delta) \varepsilon_{\mathrm{mf}} u_{\mathrm{e}} T^{\mathrm{e}} = [\delta u_{\mathrm{b}} + (1 - \delta) \varepsilon_{\mathrm{mf}} u_{\mathrm{e}}] \bar{T}_{\mathrm{p}}(1) \tag{31}$$

Whence we have

$$\bar{T}_{\mathrm{p}}(1) = a_6 T^{\mathrm{b}}(1) + (1 - a_6) T^{\mathrm{e}} \tag{32}$$

where

$$a_6 = \frac{\delta u_{\mathrm{b}}}{\delta u_{\mathrm{b}} + (1 - \delta)\varepsilon_{\mathrm{mf}} u_{\mathrm{e}}}$$

At the steady states conditions, the derivatives of the state variables with respect to time in Eqs. (13a)–(13c) are equal to zero. Therefore the steady state of the autothermal structure from Fig. 1 is described by the following set of equations

$$F(x, \lambda) = 0, \qquad F : \mathbf{R}^4_+ \to \mathbf{R}^4_+ \tag{33a}$$

where

$$x = [\alpha^{\mathrm{e}}_1, \alpha^{\mathrm{e}}_2, T^{\mathrm{e}}, T_{\mathrm{s}}(1)] \tag{33b}$$

$$F = [f_1, f_2, f_3, \psi]^{\mathrm{T}} \tag{33c}$$

whereas λ denotes a selected parameter of the model.

4. Representative results of quantitative analysis

The fundamental aim of this work was to determine the yield of the reactor for each point of operation lying on the branch of the steady states and an evaluation of the effect of the external feadback deformation. The aim of such an analysis is to select optimum operation conditions for the entire system. The yield of the reactor per unit surface area of the cross-section of the fluidized bed is determined by the expression

$$F_{\mathrm{met}} = l_{\mathrm{f}} u_{\mathrm{mf}} \rho_{\mathrm{g}} w_{\mathrm{met}} \left[\frac{\mathrm{kg\ CH_3OH}}{\mathrm{m^{-2}\,s^{-1}}} \right] \tag{34}$$

where

$$w_{\mathrm{met}} = \bar{y}_4 \frac{M_4}{\bar{M}}$$

The quantity $\bar{y}_4$ denotes the molar fraction of CH_3OH in the stream leaving the bed. It is calculated with the aid of Eq. (3), whereas weighted average conversion degrees are

$$\bar{\alpha}_i = a_6 \alpha^{\mathrm{b}}_i + (1 - a_6)\alpha^{\mathrm{e}}_i \quad (i = 1, 2) \tag{35}$$

In order to determine hysteresis loops of steady states, the local parametrization method was used for the continuation of the solution of Eqs. (33a)–(33c). System (33a) consists of four equations defining a curve in the five-dimensional (x, λ)-space. Continuation means tracing of this curve. According to Rheinboldt and Burkardt [17], the term "local parametrization" was used for the following procedure: all of the components x_i $(i = 1, \ldots, 5)$ are admitted as local parameters, including $x_5 = \lambda$. This leads to the additional equation

$$\phi(x, \eta) = x_k - \mu, \quad 1 \le k \le 5 \tag{36}$$

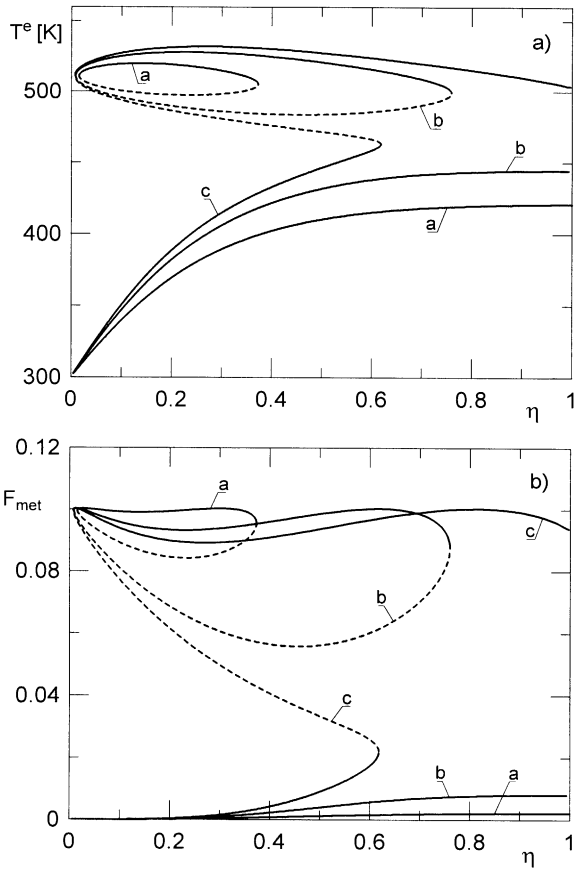

Fig. 2. Branches of steady states showing the temperature of emulsion phase T^{e} and unit yield F_{met}. (a) $T_0 = 420\,\mathrm{K}$; (b) $T_0 = 440\,\mathrm{K}$; (c) $T_0 = 450\,\mathrm{K}$ ($l_{\mathrm{f}} = 2$; $p = 50\,\mathrm{atm}$; $T_{\mathrm{f}} = 300\,\mathrm{K}$; $A_{\mathrm{q}}k_{\mathrm{q}}/S = 20\,\mathrm{kJ\,m^{-2}\,s^{-1}\,K^{-1}}$); (–) stable steady states; (- - -) unstable steady states.

with some suitable value of μ, and yields the augmented system of equations

$$F(x, \lambda) = 0 \tag{37a}$$

$$x_k - \mu = 0 \tag{37b}$$

With local parametrization, the index k and therewith the parameter is locally determined at each continuation step (x^j, η^j) [18].

For the process analysed in this work, the following composition of the feed was taken during the computations:

$$y_{01} = 0.1; \quad y_{02} = 0.06; \quad y_{03} = 0.7; \quad y_{04} = 0.14$$

All the results presented in the work were obtained for $H_{\mathrm{mf}} = 1\,\mathrm{m}$, $d_{\mathrm{z}} = 2 \times 10^{-4}\,\mathrm{m}$, $\rho_{\mathrm{z}} = 1500\,\mathrm{kg\,m^{-3}}$ and $c_{\mathrm{pz}} = 0.8\,\mathrm{kJ\,kg^{-1}\,K^{-1}}$. It was assumed that the reactor is operated adiabatically and the heat exchange occurs only in the autothermal heat exchanger.

In Fig. 2, the results of the continuation of steady states of the autothermal system are presented for $T_0 > T_{\mathrm{f}}$, i.e., for the external autothermal coupling deformation of "positive" direction.

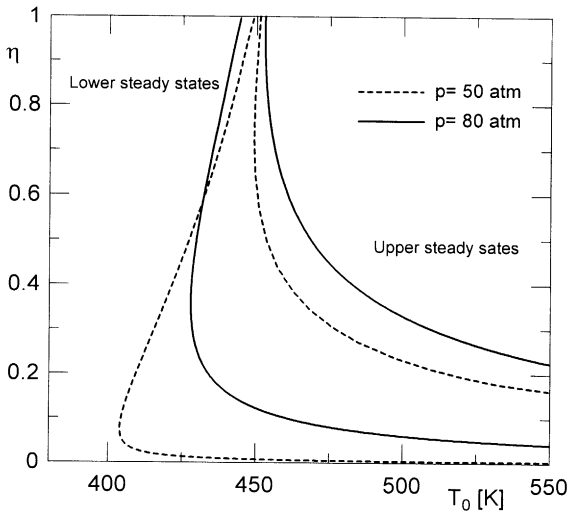

Fig. 3. Regions of multiple steady states of autothermal structure with deformed thermal feedback for two values of pressure p ($l_f = 2$; $T_f = 300\,K$; $A_q k_q/S = 20\,kJ\,m^{-2}\,s^{-1}\,K^{-1}$).

As a rule, during the non-linear analysis of steady states of non-isothermal reactors, hysteresis loops depicting the temperature of the reaction medium are presented. In Fig. 2b, the unit yield F_{met} was added, information important from the technological point of view.

It results from Fig. 2b that at each upper branch of stable steady states there exists a maximum of the yield $(F_{met})_{max}$. Let us note that for the positive direction of the autothermal coupling, all the maxima have the same value. As can be seen, as the temperature rises, they are shifted towards the higher values of the deformation degree η.

A certain number of the maximum values $(F_{met})_{max}$ lie in the area of multiple steady states and a certain number, in the area of single upper states. Therefore it should be determined for which values (T_0, η) there exist multiple and upper steady states of the studied autothermal structure. Thus the task is reduced to the continuation of the hysteresis turning points, i.e., points of the singularity co-dimension equal to one [18,19]. In Fig. 3, the results of such computations carried out for two magnitudes of the process pressure are depicted.

The literature on the calculation of turning points is rich, but differences in numerical performance of various direct methods do not appear to be significant. In this work for determining turning points, the following system of equations was used

$$F(x, \lambda) = 0 \tag{38a}$$

$$\mathbf{J}(x, \lambda) \cdot w = 0 \tag{38b}$$

$$w_k - 1 = 0 \tag{38c}$$

where w_k is a component of the vector $w = w(w_1, w_2, w_3, w_4)$ and $\mathbf{J}$ is a Jacobian matrix.

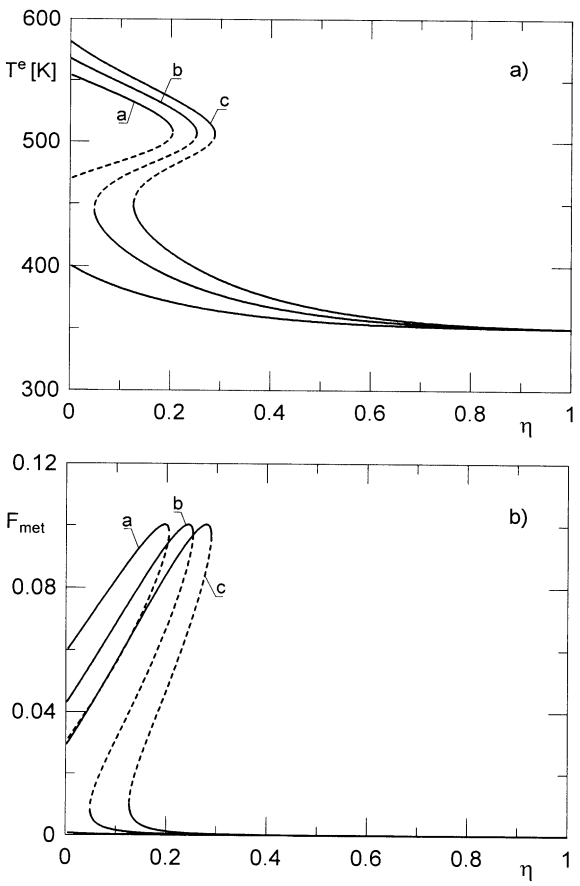

Fig. 4. Branches of steady states obtained for "negative direction" of the deformation of autothermal feedback, $T_0 < T_f$ ($l_f = 2$; $p = 50\,atm$; $T_0 = 350\,K$; $A_q k_q/S = 20\,kJ\,m^{-2}\,s^{-1}\,K^{-1}$); (–) stable steady states; (- - -) unstable steady states.

We can choose $k = 4$. Then system (38a)–(38c) consists of eight equations with respect to eight unknowns, namely: $\alpha_1^e, \alpha_2^e, T^e, T_s(1), \lambda, w_1, w_2, w_3$. At the next step one can use the algorithm of continuation, e.g., local parametrization, in order to determine the curves with the singularity co-dimension equal to 1.

The shape and the position of the region of multiple steady states depend on the pressure in the reactor. The pressure affects not only the kinetics and the equilibrium of the process but also the hydrodynamics of the fluidized bed, which had been taken into account in the computations. In other words, the mutual effect of η and T_0 depends on the pressure under which the synthesis is carried out. Let us note that for $p = 50\,atm$, the multiple, hence also the upper steady states are possible at lower temperatures T_0, which is advantageous for operational reasons.

We shall now carry out the analysis of the effect of the deformation degree for $T_0 < T_f$, i.e., for the autothermal coupling deformation of "negative" direction. The results of the relevant computations are presented in Fig. 4. They were obtained for the fixed value of T_0 and various feed temperatures T_f. As can be seen, at $T_0 < T_f$ we observe sharp

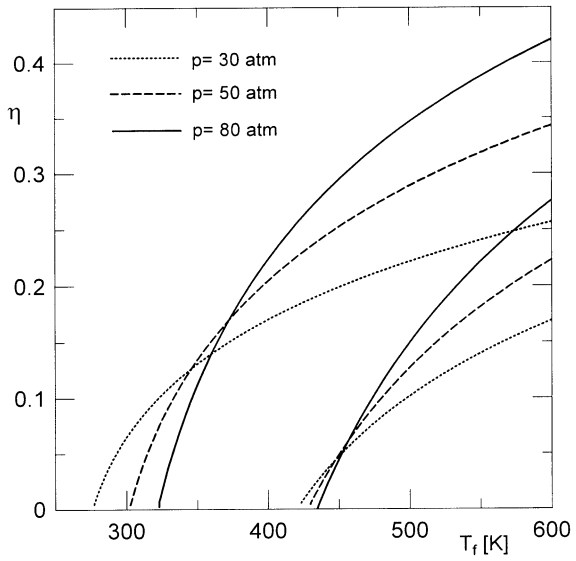

Fig. 5. Regions of multiple steady states for "negative" deformation of the external autothermal feedback ($l_f = 2$; $T_0 = 350\,K$; $A_q k_q/S = 20\,kJ\,m^{-2}\,s^{-1}\,K^{-1}$).

shapes of the curves $F_{met} = f(\eta)$. The extremum values of $(F_{met})_{max}$ lie in close proximity to turning points. It is very important information since a small exceeding of η beyond the values corresponding to $(F_{met})_{max}$ towards the greater degrees of deformation would cause the quenching of the reactor. It can, hence, be concluded that operating the plant at the deformation of "negative" direction is much more difficult than at the "positive" deformation of the external autothermal coupling.

Similarly as for $T_0 > T_f$, the continuation of the turning points of hysteresis loops was carried out. As a result, regions of multiple steady states were obtained which are presented in Fig. 5 for a few various pressures.

A natural problem which arises at studying the properties of the system presented in Fig. 1 is to evaluate the effect of the presence and the size of the heat exchanger. There arise the following questions:

1. Can a heat exchanger be selected which would ensure the maximum yield of the reactor?
2. Would the installation of an autothermal heat exchanger allow to reduce the pressure of the process? It is known though that under higher pressures reactions proceed faster, hence the rate of heat generation increases.

The answer to the first question was obtained by carrying out the continuation of steady states with respect to the parameter $A_q k_q/S$. The results of the computations are presented in Fig. 6. As can be seen, at the upper branch of steady states there is a maximum $(F_{met})_{max}$ lying, alas, in close proximity to a turning point. The higher the pressure of the synthesis, the more pronounced is the maximum.

It results from Fig. 6 unequivocally that at such a low temperature of the feed, the presence of a heat exchanger

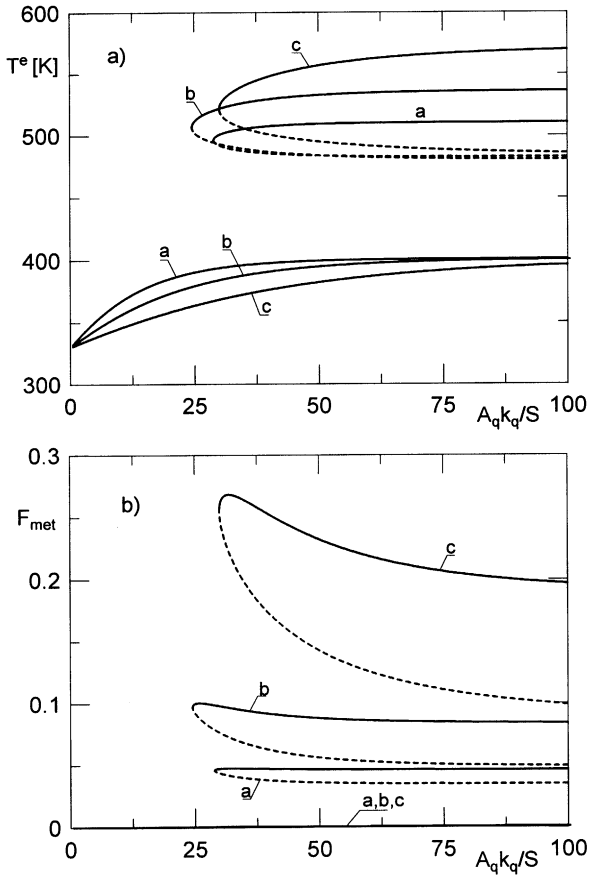

Fig. 6. Curves of steady states obtained as a result of continuation with respect to parameter $A_q k_q/S$. (a) $p = 30\,atm$; (b) $p = 50\,atm$; (c) $p = 100\,atm$ ($l_f = 2$; $T_f = 300\,K$; $T_0 = 400\,K$; $\eta = 0.3$); (–) stable steady states; (- - -) unstable steady states.

is necessary to ensure the autothermicity of the process. To answer the second of the questions posed before, the regions of multiple steady states should be determined and their boundaries plotted in the co-ordinate system ($A_q k_q/S$, p) examined. The results of appropriate computations are illustrated in Fig. 7. Each of the curves in this figure are a projection of points of the singularity co-dimension $k = 1$ onto a plane ($A_q k_q/S$, p).

For moderate pressures under which methanol synthesis is carried out, the lower boundaries of the region of multiple steady states run almost horizontally. It means that the increase in the $A_q k_q/S$ parameter does not make it possible to reduce the pressure of the process.

It results from Fig. 7 that the region of multiple steady states reaches very high pressures, not employed at the low pressure synthesis. Such high values of p are kept in the figure only by the reason of illustration since a singular point of the singularity co-dimension $k = 2$, i.e., the cusp point catastrophe, lies just in the area of high and not low pressures.

Since the pressure affects not only the proceeding of the chemical reaction but also the hydrodynamics of the bed,

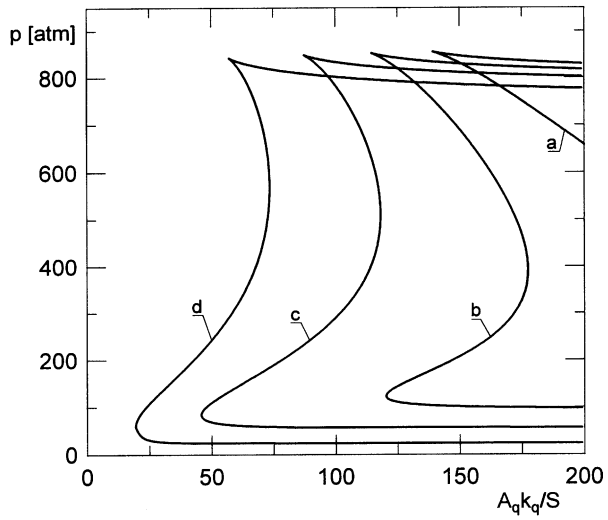

Fig. 7. Regions of multiple steady states presented in (A_qk_q/S, p) coordinates. (a) $T_0 = 300\,K$; (b) $T_0 = 320\,K$; (c) $T_0 = 350\,K$; (d) $T_0 = 400\,K$ ($l_f = 2$; $T_f = 320\,K$; $\eta = 0.3$).

the continuation computations of the steady states with respect to the parameter p were carried out. The results are presented in Fig. 8. Similarly as in Figs. 2b, 4b and 6b, also in this case there occur maximum production capacities of the reactor $(F_{met})_{max}$. In Fig. 8b we notice "sharp" maxima, though the shapes of the loops $T^e(p)$ do not indicate that, since their shape is close to horizontal. It appears that the pressure affects the reactor yield very strongly and the value of $(F_{met})_{max}$ lies very close to a turning point, crossing of which would cause a leap to the lower steady state and the quenching of the reactor. Therefore it can be said that the effect of the pressure on the yield F_{met} is not only non-linear but also discontinuous.

The last problem discussed in the present work is the evaluation of the effect of the presence and the size of the autothermal heat exchanger on the possibility to lower the feed temperature. To do such an analysis it should be determined how the boundaries of the regions of multiple steady states in the plane (A_qk_q/S, T_f) are formed. Lower and upper boundaries of the mentioned areas are denoted in Fig. 9 by Ω_1 and Ω_2, respectively. If the inequity

$$\frac{d\Omega_1}{dA_qk_q} < 0 \tag{39}$$

is observed then increasing the size of the autothermal heat exchanger makes it possible to use the feed of a lower temperature. It results from Fig. 9 that the condition (39) is observed in the entire region A_qk_q/S and for each value of the pressure p taken into account in the computations. With a sufficiently large heat exchanger, the feed of arbitrarily low temperature, limited only by technological reasons, can be employed. In other words, the application of an external heat exchanger in fluidized-bed reactors to improve their autothermicity is entirely justified.

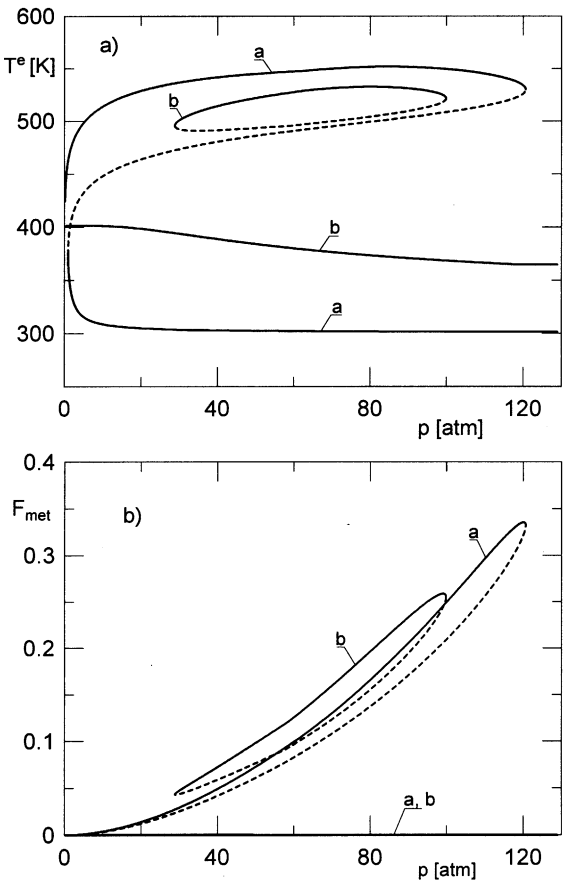

Fig. 8. Results of continuation of the steady states with respect to pressure p. (a) $\eta = 0.005$; (b) $\eta = 0.3$ ($l_f = 2$; $T_f = 300\,K$; $T_0 = 400\,K$; $A_qk_q/S = 30\,kJ\,m^{-2}\,s^{-1}\,K^{-1}$); (–) stable steady states; (- - -) unstable steady states.

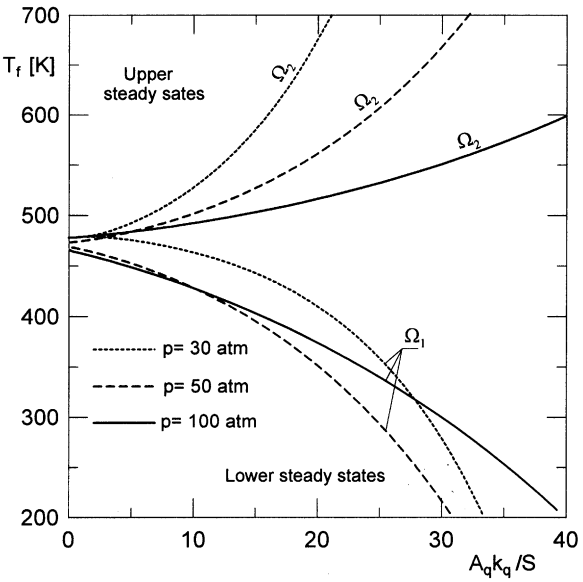

Fig. 9. Regions of multiple steady states plotted in the (A_qk_q/S, T_f) plane for several values of pressure.

5. Conclusions

Installing an external heat exchanger to preheat the feed stream before entering the fluidized-bed reactor creates new autothermal structure. Such a system is characterised by the existence of both the internal and external channels of thermal feedback. It was demonstrated that the presence of a heat exchanger definitely changes the structure of steady states of the reactor. The size of the heat exchanger was presented in the work by a complex $A_q k_q/S$ and not directly by the magnitude of the heat exchange surface area A_q. Such an approach is more advantageous when the apparatus scale is being changed.

The presence of an external heat exchanger improves the autothermicity of the entire system and makes it possible to use the feed of arbitrarily low temperature. The criterion of the "autothermicity improvement" expressed in the work by the inequality (39) has a general meaning and can be extended to other parameters of the model in the following way:

$$\frac{d\Omega_1}{d\lambda} < 0$$

where Ω_1 is the catastrophe set of singularity co-dimension $k = 1$, separating the region of multiple steady states from the region of singular lower steady states and λ is a selected parameter of the model.

A great deal of attention was focused on the phenomenon of the deformation of the external autothermal coupling. The effect of the degree and the direction of the deformation on the structure and stability of steady states as well as the yield of the reactor was investigated.

An interesting conclusion of technological and economical significance is the existence of the maximum of the yield. Equally important is the position of this maximum and the shape of the function $F_{met} = f(\lambda)$ in proximity to the maximum $(F_{met})_{max}$. It was demonstrated that the maximum of the yield lies in the upper branch of steady states, in the close proximity to a turning point. It means that $(F_{met})_{max}$ is in the region of multiple steady states. Only at the positive direction of the deformation of external coupling, i.e., when $T_0 > T_f$, the maximum yield $(F_{met})_{max}$ can be shifted to the region of singular upper steady states but only for sufficiently high temperatures T_0 (Fig. 2).

The position of $(F_{met})_{max}$ in the proximity of a turning point is significant for the operation of the plant. Incompetent attempts to reach $(F_{met})_{max}$ can lead to a change in the system operation conditions to the lower steady state and to the quenching of the reactor.

The results obtained in this work can serve as a basis for the rational selection of the process conditions of the autothermal structure analysed.

References

[1] S.S. Özturk, Y.T. Shah, W.D. Deckwer, Comparison of gas and liquid phase methanol synthesis processes, Chem. Eng. J. 37 (1988) 177.
[2] K.R. Westerterp, M. Kuczyński, A model for a countercurrent gas–solid–solid trickle flow reactor for equilibrium reactions. The methanol synthesis, Chem. Eng. Sci. 42 (1987) 1871.
[3] K.M.V. Busshe, S.N. Neophytides, I.A. Zolotarski, G.F. Froment, Modelling and simulation of the reversed flow operation of a fixed-bed reactor for methanol synthesis, Chem. Eng. Sci. 48 (1993) 3335.
[4] D. Kodra, J. Levec, Liquid phase methanol synthesis: comparison between trickle-bed and bubbe column slurry reactors, Chem. Eng. Sci. 46 (1991) 2339.
[5] S.S. Elnashaie, S.S. Elsishini, Modelling, Simulation and Optimization of Industrial Fixed-bed Catalytic Reactors, Gordon and Breach, Amsterdam, 1993.
[6] K.M. Wagialla, S.S. Elnashaie, Fluidized-bed reactor for methanol synthesis. A theoretical investigation, Ind. Eng. Chem. Res. 30 (1991) 2298.
[7] B. Tabiś, Analysis of methanol synthesis in a fluidized-bed reactor, Inż. Chem. Proc. 15 (1994) 281.
[8] B. Tabiś, A. Georgiou, Nonlinear stationary properties of a fluidized-bed autothermal system for methanol synthesis, Inż. Chem. Proc. 16 (1995) 15.
[9] S.S. Elnashaie, S.S. Elsishini, Dynamic Modelling, Bifurcation and Chaotic Behaviour of Gas–Solid Catalytic Reactors, Gordon and Breach, Amsterdam, 1996.
[10] A.A.C.M. Beenackers, G.H. Graaf, E.J. Stamhuis, The synthesis of methanol, in: Handbook of Heat and Mass Transfer, Vol. 3, Catalysis, Kinetics and Reactor Engineering, Gulf Publishing Company, Houston, TX, 1989.
[11] M. Takagawa, M. Ohsugi, Study on reaction rates for methanol synthesis from carbon monoxide, carbon dioxide and hydrogen, J. Catal. 107 (1987) 161.
[12] B. Tabiś, R. Grzywacz, Quantitative analysis of coupled fluidized-bed reactors, Inż. Chem. Proc. 14 (1993) 581.
[13] D. Kunii, O. Levenspiel, Bubbling bed model, Ind. Eng. Chem. Fundam. 7 (1968) 446.
[14] D. Kunii, O. Levenspiel, Fluidization Engineering, Wiley, New York, 1969.
[15] H. Kobayashi, F. Arai, N. Tzawa, T. Miya, Performance of gas–solid fluidized bed catalytic reactor, Chem. Eng. Jpn. 30 (1966) 656.
[16] T.E. Broadhurst, H.A. Becker, Onset of fluidization in slugging beds of uniform particles, AIChE J. 21 (1975) 238.
[17] W.C. Rheinboldt, J.V. Burkardt, A locally parametrized continuation process, ACM TOMS 9 (1983) 215.
[18] R. Seydel, Practical Bifurcation and Stability Analysis, Springer, New York, 1994.
[19] T. Poston, I. Stewart, Catastrophe Theory and its Applications, Pitman, London, 1978.